Two-dimensional GPR modeling for Hidrogeology and environmental studies

Jadir da Conceição da Silva*, UFRJ – Depto. de Geologia, Abel Carrasquilla, UENF - LENEP

Abstract

We have developed a finite element algorithm to simulate a Ground Penetrating Radar (GPR) survey responses in a two-dimensional (2D) media. The scalar TE mode of Maxwell´s wave equation is used to help us to analyze effects such as antenna frequencies selection, karst cavities detection in limestone, and pipe and buried tanks locations. Several pipes configurations are studied, mainly those filled with fresh water, salt water, oil and air. Thus, we show how efficient GPR electromagnetic method is to map groundwater conditions and their benefits to hydrogeology studies. The obtained results allow us to select optimal parameters and conditions to provide more information, which can help us, potentially, to perform the better field surveys and, consequently, to obtain better interpretations.

Introduction

The most important goal in a GPR survey is to clearly define the target depth, geometry and its electrical properties. The host material must also be qualified because it controls by contrast the degree and spatial scale of heterogeneity in the electrical properties of the model (Brewster, 1993). Other major factor in the success of a GPR survey is the selection of correct antenna frequency (Davis & Annan, 1989). In this work we have developed a 2-D finite element algorithm to simulate the scalar wave equation concerned with TE electromagnetic field mode (Fisher et al., 1992). In a first stage, we used developed algorithm to demonstrate the capability of GPR to locate pipe and buried tanks. As an option to a more complete analysis of the GPR applicability, several configurations of pipes are studied, like pipe transporting fresh water, salt water, oil, or even empty (free-air filled). Secondly, we studied the effects of different antenna frequencies used on a same site, showing that a proper antenna frequency can affect the outcome of all GPR surveys. Detection of karst cavities in limestone rock for construction planning was the next studied case, which can be filled with air or water. Finally, we model how GPR can efficiently map water table conditions, which has benefits for groundwater prospecting and contaminant hydrogeology studies. We have concluded that the target size and conductivity change the hyperbolic shape of the GPR response and the shape of the tails gives a measure of velocity and depth.

Theory

The relationship between the electric field components and their associated magnetic field components is described by the Maxwell´s equations for electromagnetic wave propagation. We know that there are two orthogonal polarizations of these fields: (a) the transverse electric (TE) mode with field components E_y, H_x and H_z; and, (b) the transverse magnetic (TM) with field components E_x, E_z and H_y. In our 2-D simulations, the fields are limited to the *x*-*z* plane, and we have opted for the TE mode. In this case, the Maxwell´s equation is reduced to the following scalar wave equation:

$$\frac{\partial^2 E_y}{\partial x^2} + \frac{\partial^2 E_y}{\partial z^2} = \mu\,\varepsilon \frac{\partial^2 E_y}{\partial t^2} + \mu\sigma \frac{\partial E_y}{\partial t} + J_y, \qquad (1)$$

which does not have an exact solution and it has to be solve by numerical methods. In Equation (1), E_y is the y-component of the electric field intensity in V/m, μ is the permeability of the medium in H/m, ε is the permittivity in F/m and σ is electrical conductivity in S/m. The term J_y represents the line external source simulating the transmitter antenna of GPR equipment. The physical property values of σ and dielectric constant k ($k = \varepsilon/\varepsilon_0$, where $\varepsilon_0 = 8{,}85\text{x}10^{-12}$ F/m is the free air permittivity) used in this work are shown in Table 1.

Table 1: Electrical and dielectric physical properties

Dielectric Constants and Electrical Conductivities of different materials		
MATERIAL	**$k = \varepsilon/\varepsilon_0$**	**σ (mS/m)**
Dry Sand	4,2	0,01
Saturated Sand	25,3	0,6
Limestone/Dolomite	6,0	0,8
Shale	11,5	40,0
Free-air	1,0	0,0
Fresh Water	80,0	0,5
Salt Water	80,0	2000,0
Oil	7,4	0

The main parameter derived from GPR method is the reflection coefficient (R), which is related with the physical properties of the media. For a particular situation of two layers, this coefficient can be express in the following form:

$$R = \frac{\sqrt{\sigma_1 + i\omega\varepsilon_1} - \sqrt{\sigma_2 + i\omega\varepsilon_2}}{\sqrt{\sigma_1 + i\omega\varepsilon_1} + \sqrt{\sigma_2 + i\omega\varepsilon_2}}. \qquad (2)$$

On the other hand, to solve the equation (1), we use a finite element numerical approach. General considerations regarding this mathematical technique indicate us that the studied region is basically subdivided in a set of triangular elements, constituting the finite element mesh (FEM) (Davies, 1980). In this form, the y-component of electrical field is approximated within each of these elements by a linear interpolation function. The goal of the FEM is to minimize the error between interpolated and true electric field intensity. To perform this error minimization it is necessary to force the inner product between the error and a test function be zero over the region where the local base function is defined. Mathematically, this means that the error is orthogonal to the test function into the sub-domain. Among several strategies to built approximated solutions of the boundary values problems like that suggested by equation (1), we have chosen the *Galerkin* method where the base and test functions are equal. So, the norm $||\varepsilon||$ is minimized by this method under assumption that temporal interval Δt must be small enough to make each iteration of the solution convergent and stable (Oden and Reddy, 1976).

Results and discussions

In all GPR survey examples discussed bellow, the data were acquiring using reflection mode with 0.50 meters transmitter-receiver antennas separation. This mode is deployed using one stack at 0.25m step intervals.

First tested geological model is showed in Figure 1(a), and Figure 1(b to e) demonstrates GPR capability to locate pipes utilities underground. Due to its high resolution, GPR allows detection of closely spaced pipes filled with different fluids, as is shown in Figure 1 (b to e). In theses figures it is possible to observe that there are some reflections of the targets when dolomite is a host rock, but any with shale, and, much better in dry and saturates sand. In this last case, it is possible to separate clearly the hyperbole reflections related to each pipe in each depth level. The presence of water with high permittivity in porous media explains these better reflection coefficients. The air and direct waves are also showed in these figures.

Second case is showed in Figure 2(a). The results present in the Figures 2(b), 2(c), 2(d) and 2(e) present the effect of different antenna frequencies used on a same site. This test has as objective to help us in the selection of an optimal frequency to perform the survey. The antenna frequencies utilized were 50 MHz (Figure 2b), 100 MHz (Figure 2c), 200 MHz (Figure 2d) and 400 MHz (Figure 2e). Thus, regarding these results, the best functioning frequency is 50 MHz, where the reflections of the three targets are clearer than the others frequencies.

Figures 3 (a, b and c) show how GPR survey is a good enough to detect cavities in karstics (limestone) rocks. As this kind of rock is almost transparent to GPR signals, all cavities filled with air give strong reflection coefficient signals for both 50 and 100 MHz antennas. The results indicate that open cavities of different geometries and sizes have different GPR signals depending upon their depth. Also, the reflection hyperboles are clearer in the case of 50 MHz than 100 MHz.

Results of Figures 4(a, b and c) show that with GPR it is possible efficiently to map the water table and its topography. Note that, for the depth indicating the water table shows much stronger reflection coefficient when data set is collected with 50 MHz antennas than 100 MHz. Some signals observed below the water table can be related with diffractions of the signal at the corner over dipping interface. Many of these effects are not noted with the 100MHz antenna due to reduced signal amplitude.

Conclusions

We have concluded, in this work, that proper antenna frequency can affect the outcome of all GPR survey. The target size and conductivity change the hyperbolic shape of the GPR response and the shape of the tails gives a good idea of media velocity and target depth. Open cavities of different geometries and sizes have distinct GPR signals depending upon their depth, which help their interpretations. It is possible to say that GPR data can perfectly distinguish geometry of the targets and our program can be used to detect different kinds of targets related with hydrogeology and environmental studies, giving a possibility to simulate different situations before to perform the field surveys. Finally, we have demonstrated that finite element method is an accurate and computationally efficient method to develop a wave equation based forward modeling algorithm for GPR applications that includes arbitrary spatial distributions of dielectric permittivity and electrical conductivity.

Acknowledgments

Both authors thank LENEP/UENF and IGEO/CCMN by the computational time. One of the authors (AC) thanks CNPq for a research fellowship.

References

Brewster, M. L., 1993, Observed migration of a controlled DNAPL release by ground penetrating radar, M.Sc. Thesis, University of Warteloo.

Davies, A. L., 1980, The finite element method: a first approach: Claredon Press.

Davis, J. C. and **Annan, A. P**., 1989, Ground Penetrating Radar for High-Resolution Mapping of Soil and Rock Stratigraphy, Geophysical Prospecting, 37, p.531-551.

Fisher, E., Mcmechan, G. A. and **Annan, A**. P.,1992, Acquisition and processing of wide aperture ground penetrating radar data, Geophysics, 57, 4, p.495.

Oden, J. T., and **Reddy, J. N**., 1976, An introduction to the mathematical theory of finite elements: John Wiley & Sons.

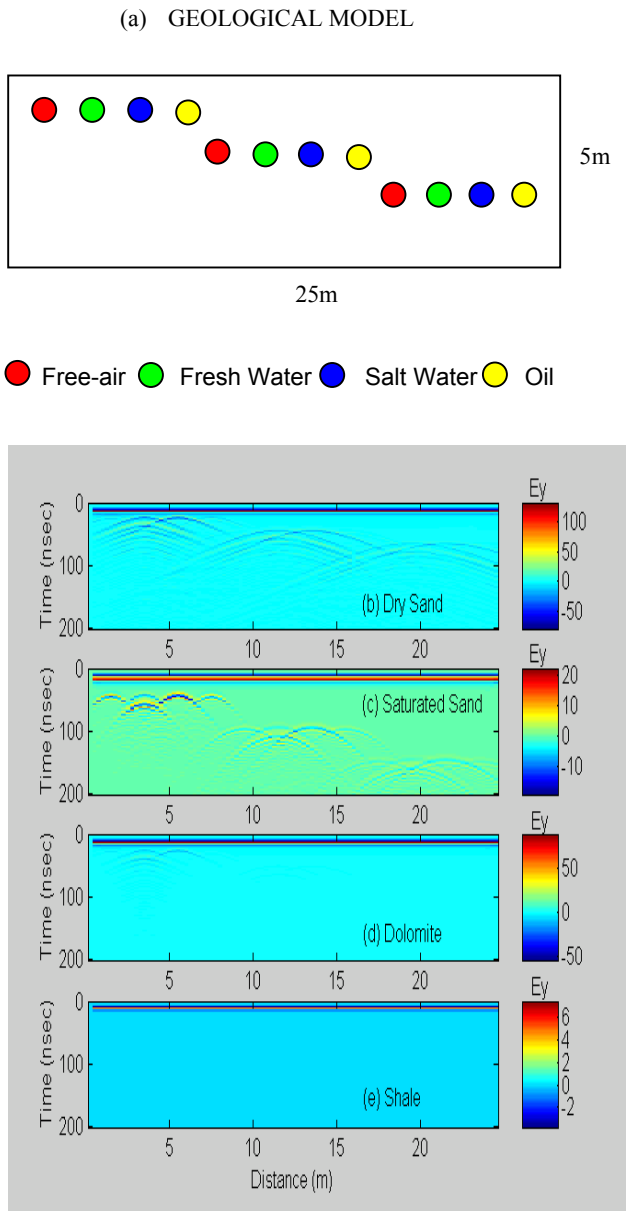

Figure 1. Study of the ability of GPR to locate pipes in different host media; (a) Geological model; (b) dry sand; (c) saturated sand; (d) dolomite and (e) shale. Each pipes set is located at 1m, 2.5m and 4m in depth and are filled with free-air, fresh or salt water and oil.

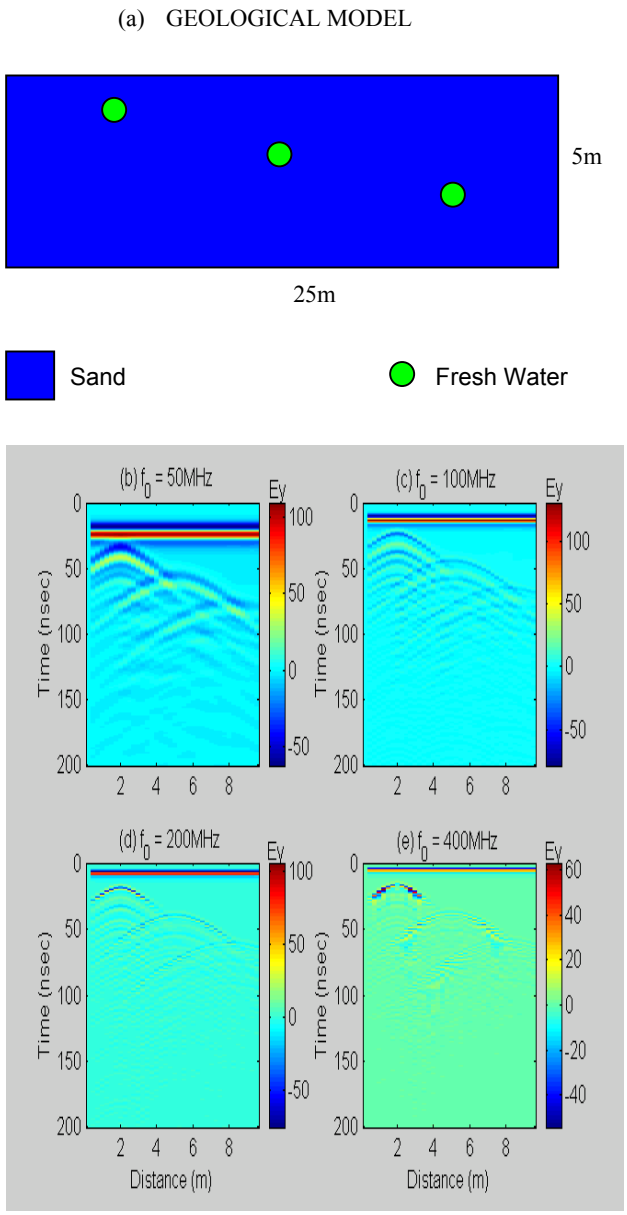

Figure 2: GPR frequency effects in buried pipes locations. (a) Geological model. The antenna frequencies used are (b) 50MHz, (c) 100MHz, (d) 200MHz and (e) 400MHz.

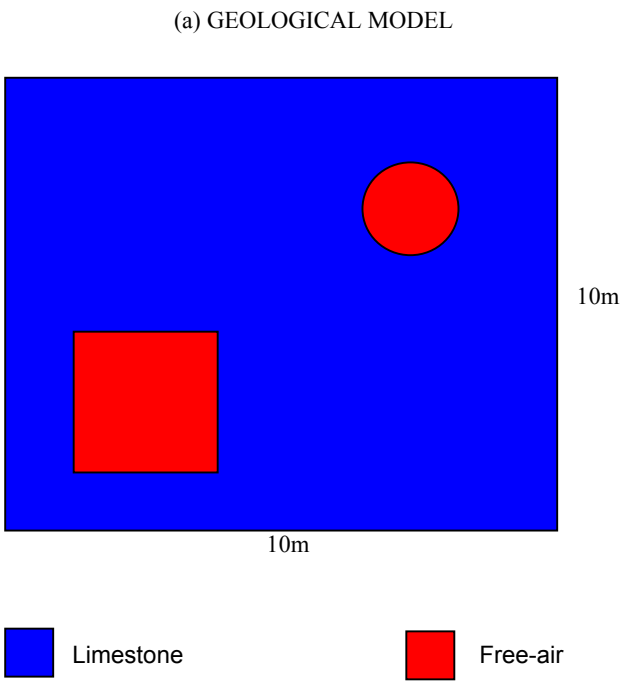

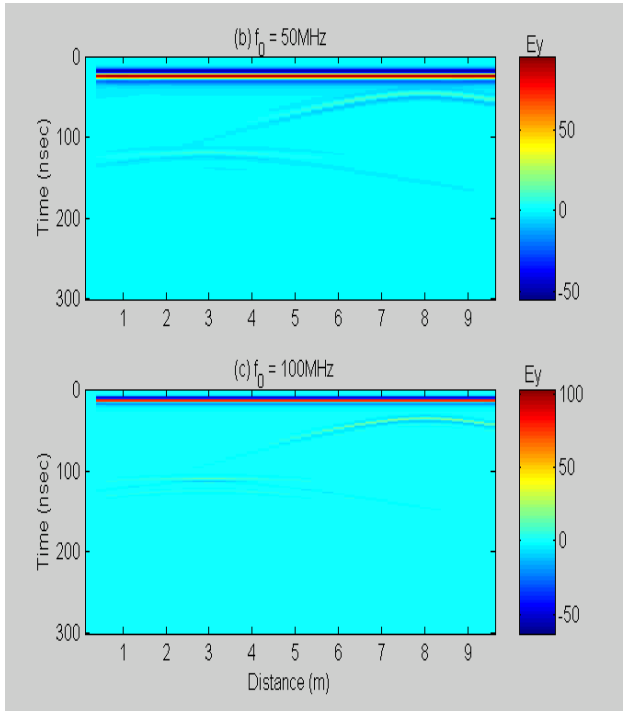

Figure 3: GPR signals of karstic cavities in limestone. (a) Geological model; (b) 50MHz and (c) 100MHz antennas. The top of the 1 meter diameter cylinder is at 2.5m and that of the 2mx2m squared cavity is 6m.

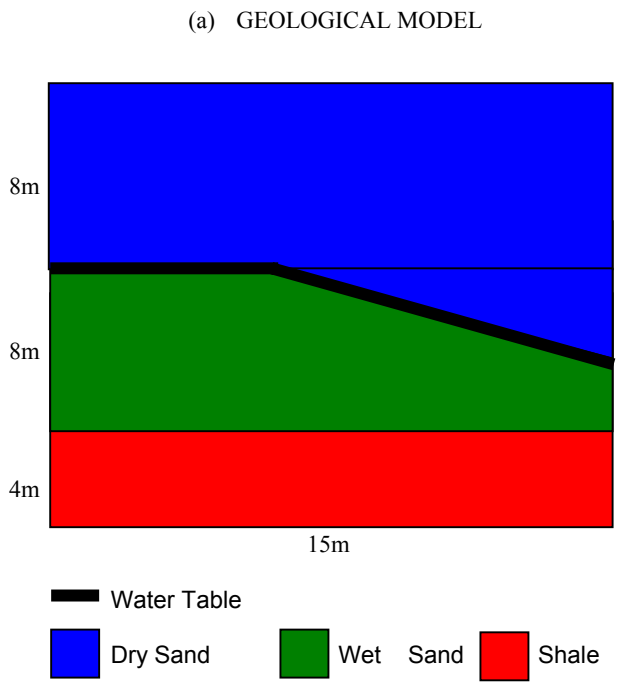

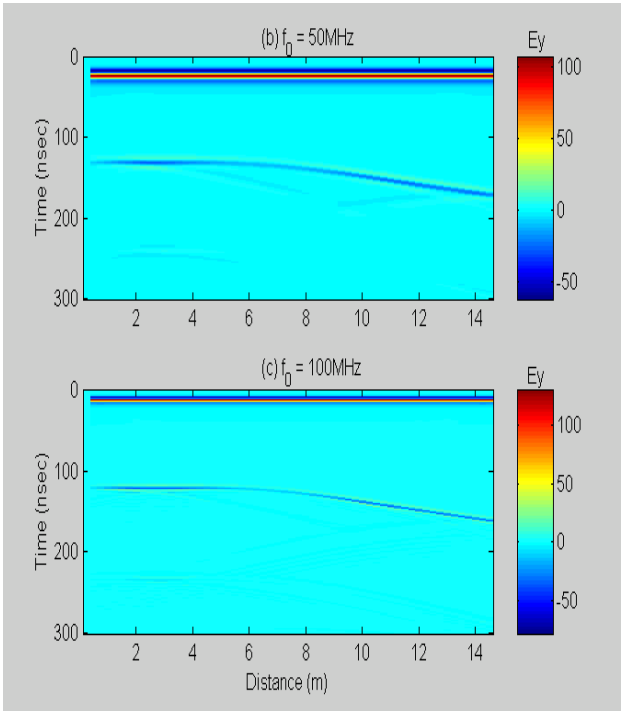

Figure 4: Water table mapping of (a) Geological model; by using frequencies of (b) 50MHz and (c) 100MHz. One can observe much stronger reflection coefficient when data set is collected with 50 MHz antennas than 100 MHz